Application of Residual Distribution (RD) schemes to the geographical part of the Wave Action Equation

Aron Roland

Institute for Hydraulic and Water Resources Engineering,

Technische Universität Darmstadt, Germany

Abstract

The framework of Residual Distribution schemes (RD) was applied to the geographical advection part of the Wave Action Equation (WAE). The schemes proved robustness, accuracy and efficiency in many different applications, ranging from Open Ocean, Coastal Seas and Laboratory Experiments. The schemes are of 1st up to 2nd order in space and time. Here the theoretical framework for these schemes is given and numerical experiments have been carried out for certain cases where an analytical solution can be easily constructed.

1. Introduction

Unstructured mesh methods have gained in the spectral wave modelling community strong influence since the early works of Benoit et al. (1996), Ardhuin (2001) and Liau (2001). Following this a variety of unstructured mesh methods have been introduced, mostly for the Eulerian form of the WAE. The method's used are mostly from the class of FE (Finite Elements) or FV (Finite Volume). As alternative to actually available numerical schemes for the solution of the geographical part in the WAE on unstructured meshes, Residual Distribution Schemes (RD; also known as *"Fluctuation Splitting Schemes"*) have been considered here.

The RD-schemes are a quite new and lovely family of numerical schemes which borrow ideas from the FE and FV framework. As a result, compact schemes and accurate solutions can be achieved on the framework of the philosophy of fluctuation splitting. Abgrall (2006) gives a recent review on the history and future trends of fluctuation splitting schemes. The Residual Distribution technique was first introduced by Roe (1982) and further improved by many other scientists (e.g. Abgrall, Deconinck, Roe, Hubbard and others).

2. Residual Distribution (RD) Schemes

As a starting point, the RD-philosophy will be briefly introduced starting from the linear advection equation. The linear advection equations for the WAE or for any scalar quantity in a divergence free flow reads:

$$\frac{\partial N}{\partial t} + \boldsymbol{c}_{\boldsymbol{x}} \nabla_{\boldsymbol{x}} N = 0 \tag{1}$$

This form of the advection equation is valid for deep water waves that are not interacting with the bottom or the ambient currents. The derivation of the RD-schemes for the flux form of the WAE (eq. 2) is shown hereinafter.

$$\frac{\partial N}{\partial t} + \nabla_X \left(\boldsymbol{c}_X N \right) = 0 \tag{2}$$

Eq.1 can be integrated by isolating the time derivative and integrating over the whole domain **Ω**.

$$\int_\Omega \frac{\partial N}{\partial t} dA = \int_\Omega \mathrm{c_g} \nabla N dA, \tag{3}$$

where the domain Ω is divided into a triangular mesh with a conformal triangulation (see Figure 1 and 2). A cell is defined with its vertices i that are numbered counter clock wise and have unique coordinates *(xi,yi)*. The discrete solutions are stored at the vertices of the triangulation. Eq. 3 can be rewritten as the sum of the integrals over each triangular cell *N*.

$$\int_\Omega \frac{\partial N}{\partial t} dA = \sum_{i=1}^{N} \int_T \frac{\partial N}{\partial t} dA \tag{4}$$

The integral on the right hand side of eq. 4 can be reformulated with the aid of eq. 3 as

$$\int_T \frac{\partial N}{\partial t} dA = -\int_T \boldsymbol{c}_X \nabla N dA = \Phi_T \tag{5}$$

Here “the integral of the time derivative over the cell is equal the fluctuation of that cell” (cf. Tomaich, 1995). The “total fluctuation” of a cell or “the residual of a cell” is named ΦT. For evaluation of these integrals over a triangular cell a distribution function within a cell for the unknown quantity must be assumed. In the fluctuation-splitting framework, usually a linear variation of the dependent variable within the triangular cell is assumed resulting in a linear basis function in every triangular element.

The approximate solution of the unknowns can be expressed as

$$\tilde{N}_{(t,x,y)} = \sum_{i=1}^{3} w_{(x,y)} \cdot N_{(t)i}, \tag{6}$$

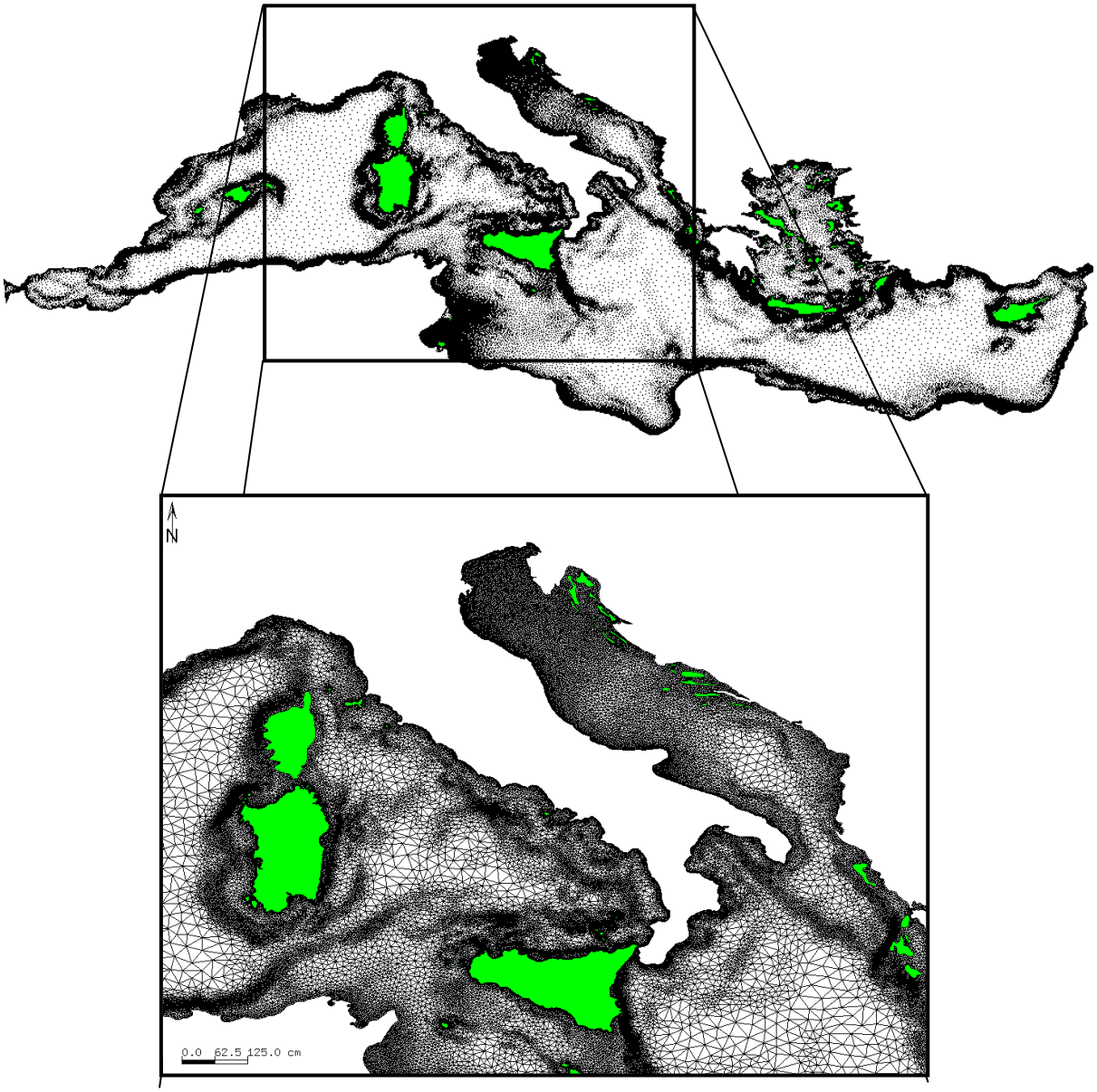

Figure 1: Example of a typical triangulated domain Ω (here the Mediterranean Sea).

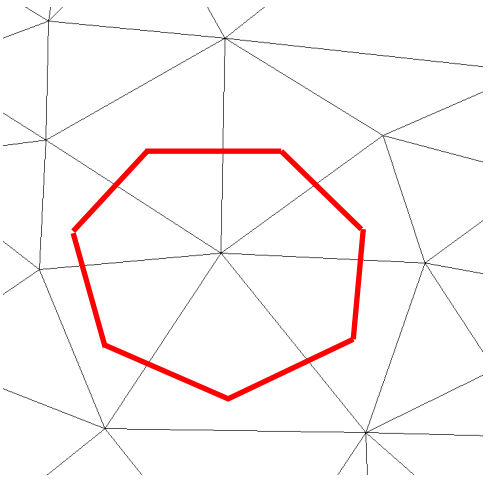

Figure 2: Typical element patch (think black line) and corresponding median dual cell (red thick line).

where w_i are the linear basis functions (see Figure 3) defined at each vertex. The RD-schemes borrows at this stage the idea from the Finite Element Method, see e.g. Donea (1985), eq. 6 is similar to his eq. 7. The total cell fluctuation (eq.5) can now be written in a discrete form introducing the spatial derivative of wave action, which is given for a linear basis function, w_i within the element as:

$$\nabla N = -\frac{1}{2S_T}\sum_{i=1}^{3} N_i \boldsymbol{n_i} \tag{7}$$

Substituting eq.7 in the right hand side of eq.5 one can rewrite the total fluctuation as follows:

$$\begin{aligned} \Phi_T &= -\int_T \boldsymbol{c_X} \nabla N dA \\ &= \sum_{i=1}^{3} \frac{1}{2}\lambda \cdot N_i \cdot \boldsymbol{n_i} = \sum_{i=1}^{3} N_i \left(\frac{1}{2}\lambda \cdot \boldsymbol{n_i}\right) = \sum_{i=1}^{3} k_i N_i \end{aligned} \tag{8}$$

ST is the area of the triangle and ni the edge normal vector defined according to Figure 3. The vectors $\mathbf{n}_i$ are scaled with the edge length to opposite to its vertices. λ is the linearized advection vector of the cell. In this special case it was assumed that it is constant in spatial space (no currents, deep water) so it follows that:

$$\lambda = \frac{1}{3}\sum_{i=1}^{3} \boldsymbol{c_{X,i}} = \boldsymbol{c_{X,i}} \text{ for } \boldsymbol{c_{X,i}} \neq \boldsymbol{c_{X,i(X)}} \tag{9}$$

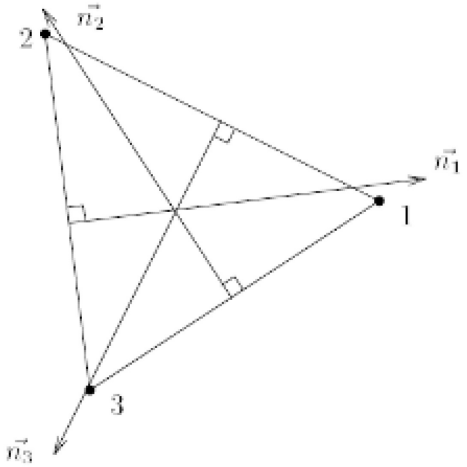

Figure 3 Definition of the edge normal vectors (adapted from Tomaich, 1995).

Introducing the scalars ki

$$k_i = \frac{1}{2}\lambda \boldsymbol{n_i} \tag{10}$$

one can see that the sum of all vectors ni is zero so that following identity is valid:

$$\sum_{i=1}^{3} \boldsymbol{n_i} = 0 \tag{11}$$

. (11)

From eq.11 immediately follows that

$$\sum_{i=1}^{3} k_i = 0 \tag{12}$$

These relationships are important for the further derivation of the RD-schemes. The total fluctuation of a triangular cell for the linear conservation law can now be rewritten using the above-defined relationships as follows:

$$\Phi_T = \sum_{i=1}^{3} k_i N_i = \sum_{i=1}^{3} \alpha_i \Phi_T = \sum_{i=1}^{3} \Phi_{i,T} \ , \tag{13}$$

αi are the redistribution coefficients, which must be in their sum unity in order to guarantee conservation,

$$\sum_{i=1}^{3} \alpha_i = 1 \tag{14}$$

Si is the median dual cell area (see Figure 2), which can be evaluated as the sum of one third of the cell areas Ai connected to the certain vertex i.

$$S_i = \sum_{i=1}^{N_{con.}} \frac{1}{3} \cdot A_i \tag{15}$$

The numerical approximation of eq.1 is then obtained through the following explicit “finite volume type” time integration procedure.

$$N_i^{n+1} = N_i^n + \frac{\Delta t}{S_i} \sum_{T, i \in D_i} \Phi_{i,T} \tag{16}$$

In order to update the solution, the contribution of all fluctuations Φi,T, that are members of the set of triangles Di (element patch) connected to node I, are cumulated. The cumulated cell fluctuations are weighted by the area of the median dual cell, which results in an updating scheme, which is very similar to cell-vertex FV-schemes (e.g. Qian et al. 2007). However, one advantage of the above described updating procedure is that for FV-schemes the nodal update is calculated as the sum of the edge fluxes defining the median dual cell, which are twice more than cells needed for the update in the FS scheme. The sum of all nodal fluctuations, contributing to the nodal update, vanishes when eq.16 reaches its steady state solution:

$$\sum_{T,i\in T_i} \Phi_{i,T} = 0 \tag{17}$$

After the total fluctuation of a certain cell has been calculated, it must be distributed over the vertices of the cell. The main problem in designing the schemes lies in the definition of the redistribution coefficients αi, which characterizes the final advection scheme. Certain design principles are defined in order to develop proper redistribution schemes. These criteria are

Conservation or property (C) requires that the solution at the new time level n+1 conserves the depended variable. This is guaranteed as long as the distribution coefficients αi in eq.14 are in their sum unity.

Positivity of the scheme, or the so called property (P). For a linear scheme, the solution at the new time level can be written as sum of the product between the coefficients $\tilde{c}_k$, resulting from the discretization of a certain scheme. The values of the updated solution are positive if the coefficients $\tilde{c}_k$ are positive

$$u_i^{n+1} = \sum_{k=1}^{N} \tilde{c}_k \cdot u_k^n \tag{18}$$

For explicit schemes this condition is normally strictly connected to a CFL stability criterion, which must be maintained in order to get stable and monotone solutions. For the explicit schemes, in the RD-framework this criterion is:

$$\Delta t_i = \max_{T,i\in D_i} \left(\frac{k_i^+}{A_i} \right) \tag{19}$$

Linear Preservation (LP); Condition LP prescribes that the numerical scheme maintains 2nd order accuracy at steady state in smooth regions of the solution while retaining monotonicity in the vicinity of shocks as long the CFL-like condition is met.

Based on the "Godunov's order barrier theorem" linear schemes[1] cannot be both (P) and (LP) at the same time according to, which states that linear monotone schemes cannot be of second order without producing oscillative solutions. It is possible to construct second order linear preserving schemes, but this makes a nonlinear redistribution of the fluctuations necessary. In the framework of explicit time integration schemes, this can be done with the application of so called "Flux limiters" or with the aid of blending of linear monotone and nonlinear non-monotone schemes (e.g. Roe, Leonard and many others). In the framework of Finite Volume schemes, this is called "Total Variation Diminishing" criterion. The second order fluxes of the non-monotone schemes are limited near strong gradients, where these schemes would otherwise produce non-positive values, and monotone first order schemes are used. The art of designing such limiters is to apply them only in situations where the second order schemes lead to non-monotone results maintaining second order accuracy as often as possible. In the RD-framework, similar technique can be applied as done in e.g. by Hubbard & Roe (2002). One advantage of explicit integration schemes is that they are faster than implicit schemes because no linear equation system has to be solved. Another advantage is that nonlinear schemes can be designed

[1] Linear schemes, in the sense, that the solution at the new time level is a *linear combination* of the old values of the solution.

in order to fulfil all the above-mentioned design criteria. The results are non-oscillatory monotone higher order space/time schemes with a high accuracy.

However, in certain applications, where a high spatial resolution is needed, the limiting factor for the explicit schemes becomes the stability criterion of eq. 19. The numerical scheme can become unfeasible with respect to the needed computational time.

Implicit schemes have with respect to this a clear advantage, they can be designed in such a way that their stability and monotonicity does not depend on the CFL criterion. The price to pay is the solution of a linear equation system that evolved in the solution procedure. The computational time for the implicit scheme is roughly two times greater than for the implicit schemes for the case of the explicit and implicit N-scheme (see Roland, 2009). In order to obtain an unconditionally monotone implicit scheme that is also LP must lead, because of the Godunov theorem, to a nonlinear scheme (see e.g. Abgrall & Mezine, 2004 and Richuotto et al., 2005). The resulting equation system becomes in this case naturally also nonlinear and iterative methods have to be used for the solution. For the WAE this is a crux since the advection part must be solved for each spectral component that average around 800 -1200 quantities with different advection velocities makes an application of a nonlinear equation solver to a computationally very expensive task. In this thesis, the author did not consider nonlinear implicit schemes because of the necessary iterative solution procedure and the associated computational costs. As long as the implicit schemes are linear and monotonicity should be retained the schemes cannot be second order in space and time and though LP. Higher order linear schemes will always be limited by a CFL as condition for which monotonicity is retained. However, the author focuses in this work on linear and non-linear explicit schemes as this was the demand of the centre.

2.1. Explicit Residual Distribution schemes

2.1.1. The CRD N-scheme

The basis of all RD-schemes is the N-Scheme, which has its name because of its narrow numerical stencil as it uses only the nearest neighbour nodes to compute the nodal update of the solution. In order to describe the N-Scheme for the general nonlinear conservation law, first the scheme for a linear conservation law given by eq. 20 will be derived. The standard N-scheme can be designed introducing an upwinding for the distribution of the total fluctuation over the nodes of the elements. In order to do so, it must be distinguished between two and one-sided inflow triangles (e.g. Tomaich, 1995). The amount of inflow sides and the upwind nodes are defined through the signs of the k-values. For the simple case of one inflow side, the whole fluctuation Φ_T is sent to the upwind node. For the more complicated case of two inflow sides, the total fluctuation is split between the nodes. The method of this splitting defines the final character of the scheme. The total fluctuation can be rewritten using eq.12, for the case of two inflow edges as shown in Figure 4, as

$$\Phi_T = k_2 \cdot \left(N_2 - N_1\right) + k_3 \cdot \left(N_3 - N_1\right). \tag{20}$$

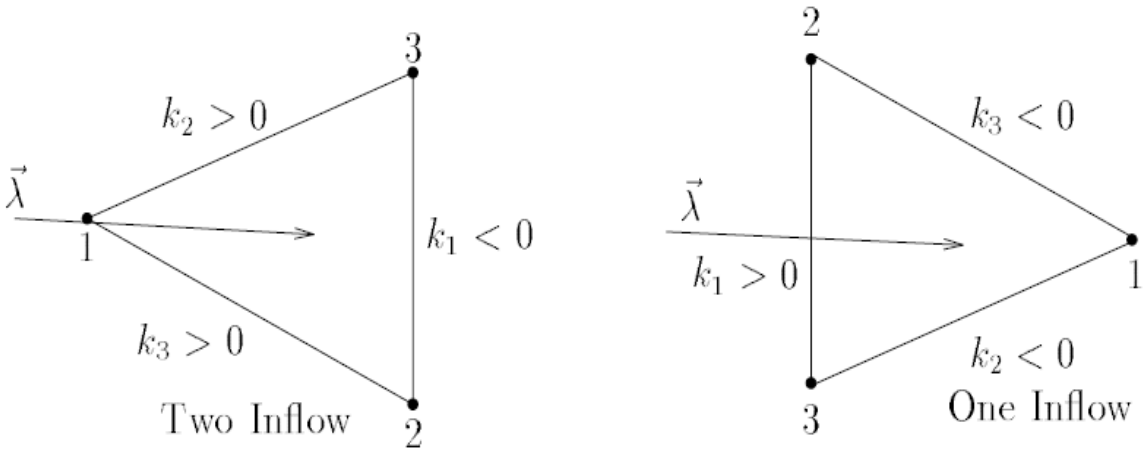

Figure 4: Two and one side inflow within a triangle; taken from Tomaich (1995)

From eq. 20 the splitting is obvious and the redistribution of the fluctuations for the N-scheme reads

$$\begin{aligned}\Phi_{1,T} &= 0 \\ \Phi_{2,T} &= k_2 \cdot (N_2 - N_1) \\ \Phi_{3,T} &= k_3 \cdot (N_3 - N_1)\end{aligned} \tag{21}$$

Following e.g. Abgrall (2006) the N-scheme can be written in a more compact form introducing positive and the negative k's

$$\begin{aligned}k_i^+ &= \max(k_i, 0) \\ k_i^- &= \min(k_i, 0)\end{aligned} \tag{22}$$

so that

$$k_i = k_i^+ + k_i^- \tag{23}$$

and the upwind residual becomes

$$\tilde{N} = \tilde{n} \cdot \left(\sum_{i=1}^{3} k_i^- N_i \right) \tag{24}$$

with

$$\tilde{n} = \left(\sum_{i=1}^{3} k_i^- \right)^{-1} \tag{25}$$

The resulting splitting for the total fluctuation may now be written as

$$\Phi_{i,T} = k_i^+ (N_i - \tilde{N}) \tag{26}$$

It can be easily seen that, when cumulating all nodal fluctuations according to eq. 27, the total fluctuation of the cell is obtained which renders the scheme a conservative one.

$$\Phi_T = \sum_{i=1}^{3} \Phi_{i,T} \tag{27}$$

The above set of equations defines the standard N-scheme for linear conservations laws according to eq. 1. The resulting scheme is valid only for the WAE in the case of the deep-water waves without ambient currents when the group velocities are divergence free in geographic space. The flux form, which is valid in the general case, is defined as

$$\frac{\partial N}{\partial t} + \nabla_{\boldsymbol{X}} \left(\boldsymbol{c}_{\boldsymbol{X}} N \right) = 0 \tag{28}$$

and can be rewritten using the product rule giving

$$\frac{\partial N}{\partial t} + \nabla_{\boldsymbol{X}} \left(\boldsymbol{c}_{\boldsymbol{X}} N \right) = \frac{\partial N}{\partial t} + \boldsymbol{c}_{\boldsymbol{X}} \nabla_{\mathrm{X}} N + N \nabla_{\mathrm{X}} \boldsymbol{c}_{\boldsymbol{X}} \tag{29}$$

Since the last term of the right hand side of eq. 29 do not vanish[2] in the general case, there is no obvious linearization for eq. 28 and therefore the conservative form must be solved given through eq. 28.

In order to construct a conservative scheme in terms of the RD-framework, Csik et al (2002) introduced the CRD-scheme (Conservative contour Integral based Residual Distribution scheme) where the total cell fluctuation is evaluated over the cell contour integrating an arbitrary flux function F with a higher order integration method for the evolving Gauss integral.

$$\Phi_T = -\oint_{\partial T} \nabla \mathbb{F} \cdot \vec{n} dS \tag{30}$$

For the WAE, the flux function is defined as

$$\mathbb{F} = \boldsymbol{c}_{\boldsymbol{X}} \cdot \mathrm{N} \tag{31}$$

For the case of the conservative form of the WAE, which is valid for general nonlinear conservation laws, the nodal residual must be calculated according to Csik et al. (2002). The authors suggested replacing eq. (24) with the following formula in order to conserve an arbitrary flux function F.

$$\tilde{N} = \tilde{n} \cdot \left(\sum_{i=1}^{3} k_i^+ N_i - \Phi_T \right) \tag{32}$$

Eq. (32) can easily be derived when rewriting eq.8 for the case of the two inflow edges and calculating the contribution of the upwind node, but with the difference that the total fluctuation Φ_T is an unknown quantity. This leads directly to eq. 33 which is equivalent to eq. 32.

[2] The solution of the linearized equations in shallow water would result e.g. in an absence of the wave shoaling.

$$N_1 = \frac{1}{k_1}\left(k_2 \cdot N_2 + k_3 \cdot N_3 - \Phi_T\right) \tag{33}$$

If the upwind contribution is calculated this way it can be seen, when cumulating all contributions from the nodes of each element according to eq.30, that the total fluctuation is conserved when using eq.32. Since the upwind contribution is now evaluated of terms of the total fluctuation Φ_T, integrating eq.30 numerically, the conservation of arbitrary flux functions F is enforced. The linearized state, defined through the average velocity in the element, is used only for the identification of the upwind direction. This procedure can be seen as a correction of the linear advection scheme for the presence of an additional nonlinear flux.

The total cell fluctuation can be calculated with aid of the Simpson integration. The Gauss integral over the triangle edges (eq.30) must be evaluated with a higher order integration scheme (e.g. Simpson Rule) because if first order schemes, such as the "Trapezoidal Rule", are used, the resulting scheme will not accurately conserve the fluctuations of the cell and may generate greater negative values in the vicinity of large gradients in the solution. The flux at the middle of each edge can be defined as the product of the average edge normal velocities and wave action densities at the nodes of each edge.

$$\Phi_T = -\oint_{\partial T} \nabla \mathbb{F} \cdot \mathrm{n} ds = \sum_{j=1}^{3} \int_{l_j} \mathbb{F} \cdot \mathrm{n}_j ds_j \tag{34}$$

The Simpson rule for one edge reads:

$$\int_{l_i} \mathbb{F} \cdot \mathrm{n} ds = \frac{l_j}{6}\left(F_\perp(a) + 4F_\perp\left(\frac{a+b}{2}\right) + F_\perp(b)\right) \tag{35}$$

$F^{\perp}$ are the edge normal fluxes at the beginning and the endpoint of the edge and are defined as:

$$\begin{aligned} F_\perp(a) &= c^\perp_{a,j} \cdot N_a \\ F_\perp(b) &= c^\perp_{b,j} \cdot N_b \end{aligned} \tag{36}$$

a and b are representing the beginning and the endpoint of the edge and the index j runs over the edges of the triangle. N_a and N_b are the wave actions and $c^\perp_{a,j}$ and $c^\perp_{b,j}$ are the advection velocities normal to the edge j at point a and b respectively.

The average wave-action-flux at the middle of the edge j is defined as with the average values of the wave action and the normal advection velocity at each node of edge j, this is the only way to allow for a weakly non-linear variation along the edge of each triangle[3].

$$F_\perp\left(\frac{a+b}{2}\right) = \frac{c^\perp_{a,j} + c^\perp_{b,j}}{2} \cdot \frac{N_a + N_b}{2} \tag{37}$$

[3] The author is thankful for the discussion with Herman Deconinck with respect to this issue.

This can be rewritten as

$$4F_{\perp}\left(\frac{a+b}{2}\right)=N_a\left(c^{\perp}_{a,j}+c^{\perp}_{b,j}\right)+N_b\left(c^{\perp}_{a,j}+c^{\perp}_{b,j}\right) \tag{38}$$

Using eq. 36 and eq. 37 one can rewrite eq. 35 as:

$$\int_{l_j}\mathbb{F}\cdot\vec{n}ds=\frac{l_j}{6}\left(N_a\left(2c^{\perp}_{a,j}+c^{\perp}_{b,j}\right)+N_b\left(2c^{\perp}_{a,j}+c^{\perp}_{b,j}\right)\right) \tag{39}$$

For all edges of a certain element this can be written in a discrete form introducing node numbers i, i+1 and i+2 for a, b and c as

$$\begin{aligned}\oint_{\partial T}\nabla\mathbb{F}\cdot\vec{n}ds=N_i&\left(\frac{l_1}{6}\left(2c^{\perp}_{i,1}+c^{\perp}_{i+1,1}\right)+\frac{l_3}{6}\left(2c^{\perp}_{i+2,3}+c^{\perp}_{i,3}\right)\right)+\\ &N_{i+1}\left(\frac{l_2}{6}\left(2c^{\perp}_{i+1,2}+c^{\perp}_{i+2,2}\right)+\frac{l_1}{6}\left(2c^{\perp}_{i,1}+c^{\perp}_{i+1,1}\right)\right)+\\ &N_{i+2}\left(\frac{l_3}{6}\left(2c^{\perp}_{i+2,3}+c^{\perp}_{i,3}\right)+\frac{l_2}{6}\left(2c^{\perp}_{i+1,2}+c^{\perp}_{i+2,2}\right)\right)\end{aligned} \tag{40}$$

With some algebra eq.40 can be expressed as

$$\Phi_T=\oint_{\partial T}\nabla\mathbb{F}\cdot\vec{n}ds=\sum_{i=1}^{3}N_i\delta_i \tag{41}$$

with

$$\begin{aligned}\delta_1&=\frac{l_1}{6}\left(2c^{\perp}_{i,1}+c^{\perp}_{i+1,1}\right)+\frac{l_3}{6}\left(2c^{\perp}_{i+2,3}+c^{\perp}_{i,3}\right)\\ \delta_2&=\frac{l_2}{6}\left(2c^{\perp}_{i+1,2}+c^{\perp}_{i+2,2}\right)+\frac{l_1}{6}\left(2c^{\perp}_{i,1}+c^{\perp}_{i+1,1}\right)\\ \delta_3&=\frac{l_3}{6}\left(2c^{\perp}_{i+2,3}+c^{\perp}_{i,3}\right)+\frac{l_2}{6}\left(2c^{\perp}_{i+1,2}+c^{\perp}_{i+2,2}\right)\end{aligned} \tag{42}$$

The coefficient δ_i depends on the velocities at the edges and the geometry of the triangle. Using eq. 41 and eq. 34, eq. 32 can be rewritten as

$$\begin{aligned}\tilde{N}&=\tilde{n}\cdot\left(\sum_{i=1}^{3}k_i^{+}N_i-\Phi_T\right)\\ &=\tilde{n}\cdot\left(\sum_{i=1}^{3}k_i^{+}N_i-\sum_{i=1}^{3}\delta_iN_i\right)\\ &=\tilde{n}\cdot\left(\sum_{i=1}^{3}N_i\left(k_i^{+}-\delta_i\right)\right)\end{aligned} \tag{43}$$

In this way, the upwind fluctuation can be expressed only with the nodal values that are functions of the geometry and the wave kinematics. This is important for the derivation of the implicit FS schemes. The CRD-N scheme has very similar characteristics as the standard N-Scheme. It is as explicit as the first order space/time scheme that is monotone under the CFL condition given in eq. 19 and conservative.

However, the presented variant of the N-scheme is quasi-positive, since for the CRD-approaches positivity cannot be proven due to the numerical integration of the flux function along the edges (Csik et al. 2002). However, the resulting scheme is monotone and the negative values are neglectable and do not alter in a practical sense the conservation of the scheme when set to zero. The above set of discrete equations describes the CRD-N scheme as it is implemented in the WWM II, WW-III and WAM.

2.1.2. The CRD-LDA (Low Diffusion Approximation) scheme

The LDA (Low Diffusion Approximation) scheme is of first order in time, second order in cross flow direction and first order in longitudal flow direction. The scheme is LP, but since it is linear, it is not positive and therefore non-monotone due to the Godunov theorem. However, the LDA-scheme is used in combination with lower order schemes (e.g. N-scheme) to design nonlinear schemes which fulfil all the above-mentioned design criteria such as the PSI (Positive Streamline Invariant) scheme or the FCT scheme using residual distribution. The nodal fluctuation of the standard LDA scheme reads for a certain element (e.g. Abgrall, 2006):

$$\Phi_{i,T} = -\tilde{n}k_i^+\Phi_T \tag{44}$$

It is easy to see that the above given scheme is conservative since the sum of the redistribution coefficients is unity when cumulated over all nodes of the element:

$$\sum_{i=1}^{3} -\tilde{n}k_i^+ = \sum_{i=1}^{3}\alpha_i = 1 \tag{45}$$

In order to formulate a contour integration based LDA scheme, the total fluctuation in eq. 44 must be replaced by eq. 41 in order to solve the conservative form of the WAE. The LDA scheme is a higher order linear scheme and therefore not positive and non-monotone. The resulting scheme achieves first order accuracy in time and second order in cross flow direction and first order in longitudal flow direction.

2.1.3. The CRD-PSI-scheme

As given in the introduction of this chapter, a scheme, which is conservative, positive, and linear preserving, must be, due to Godunov's Theorem, a nonlinear scheme. The PSI-scheme fulfils these demands and it was constructed with the aid of a blending parameter, which reduces the contribution of the higher order scheme when non-monotone solutions are present (e.g. Abgrall, 2001). The nodal fluctuation of the PSI scheme can be defined with the blending parameter according to Abgrall (2002) as:

$$\Phi_{i,T,PSI} = l\cdot\Phi_{i,T,N} + \left(1-l\right)\cdot\Phi_{i,T,LDA} \tag{46}$$

with

$$l = \max\left(\phi(r_1), \phi(r_2), \phi(r_3)\right) \tag{47}$$

and

$$r_i = \frac{\Phi_{i,T,N}}{\Phi_{i,T,LDA}}$$
$$\varphi(x) = \begin{Bmatrix} \dfrac{x}{x-1} & \text{if } x < 1, \\ 0 & \text{else,} \end{Bmatrix} \tag{48}$$

The resulting scheme is nonlinear and it was shown by several authors that the scheme satisfies the above defined design criteria. Using the CRD-N scheme and the CRD-LDA scheme, the resulting CRD-PSI holds for any conservation law as the one given through eq. 2. The scheme is first order in time and it is at its best second order in cross flow direction and first order in longitudal flow direction. The scheme is positive for a linear conservation law. The PSI scheme was used hereinafter to construct a truly second order space-time scheme, which retains the above-defined design criteria on the foundation of the CRD approach of Csik et al., 2002.

2.1.4. The CRD-FCT-LW-PSI scheme

Hubbard & Roe (2000) combined two fluctuation splitting schemes, namely the PSI scheme presented above and the non-monotone higher order Lax-Wendroff RD-scheme in order to design a monotone and positive scheme. In this thesis, the author used the concept of Csik et al. (2002) to formulate a contour integration based version of the Residual Distribution (CRD) Flux Corrected Transport scheme (CRD-FCT-LWPSI). The Lax-Wendroff scheme in the RD context reads:

$$\Phi_{i,T} = \left(\frac{1}{3} + \frac{\Delta t}{2A_i} k_i\right)\Phi_T \tag{49}$$

This was achieved with a generalized FCT approach in the context of the RD-framework. The scheme is written in a form, which isolates the cell contribution and limits the contribution of the non-monotone scheme in an optimal way near discontinuities. This is done in an optimized way in order to retain the higher order solution as often as possible. The FCT approach in the FS context can be described in four basic steps.

First, the higher (HEC) and lower order contributions (LEC) from the Lax-Wendroff and PSI scheme are computed and the difference of the node wise contribution of each scheme is estimated and defined as the so called AEC (Anti diffusive Element Contribution):

$$AEC_i = \Phi_{i,T}^{LAX} - \Phi_{i,T}^{PSI} \tag{50}$$

In the 2nd step the low order solution is calculated using eq.16 which gives then

$$N_i^{PSI,n+1} = N_i^n + \frac{\Delta t}{S_i} \sum_{T, i \in T_i} \Phi_{i,T}^{PSI} \tag{51}$$

In the third, most important step, the AEC must be corrected in such a way that the solution at the new time level is monotone. This is achieved with correction factors βi leading to:

$$AEC_{i,corr} = \beta_i \cdot AEC_i \tag{52}$$

The final update is obtained by advancing in time and adding the corrected AEC to the solution of the lower order scheme according to:

$$N_i^{n+1} = N_i^{PSI,n+1} + \frac{\Delta t}{S_i} \sum_{T,i \in T_i} AEC_{corr,i} \tag{53}$$

The main problem in such an approach is to formulate the correction factors βi which must also guarantee conservation in the case of the RD-approach. The procedure for the calculation of the correction factors is described in detail in Hubbard & Roe (2000) and will not be repeated for the sake of brevity. The author has also considered in this thesis another non-monotone scheme, which is the 2nd order upwind control volume (UCV) scheme of Paillere (1995) that reads:

$$\Phi_{i,T} = \left(\frac{1}{3} + \frac{3}{3} \frac{k_i}{\sum_{i=1}^{3} k_i^+} \right) \Phi_T \tag{54}$$

The scheme was also incorporated in the FCT approach, but the results have been not as good as for the scheme suggested by Hubbard & Roe. As the FCT scheme in this thesis was constructed on the foundation of the above described CRD schemes, the total fluctuation in was calculated numerically integrating the flux function over the element edges. The resulting scheme should be conservative for arbitrary flux functions. In fact the author did not find any situation where the opposite occurs and the schemes are used as well in the TIMOR (Tidal Morphodynamics, Zanke, 2002) for the solution of the tracer transport and the Exner equation.

2.2. Verification of the advection schemes

2.2.1. The "rotating cylinder"

In order to verify the numerical schemes the "rotating cylinder" test case was investigated, which was also used by Hubbard & Roe (2002) and used in many studies to verify the implementation and the diffusion characteristics of the scalar advection schemes. In a quadratic domain Ω = [-1,-1] – [1, 1] the advection velocity vector is given as:

$$\vec{\lambda} = \begin{pmatrix} -y \\ x \end{pmatrix} \tag{55}$$

This results in a circular current field in which the initial state is equivalent to the analytical solution after one rotation. The initial distribution of the unknown is discontinuous at the edges of the cylinder (see Fig.5) and defined as follows:

$$N = \begin{cases} 1, & \text{if } r \le 0.25 \\ 0, & \text{else} \end{cases} \tag{56}$$

with

$$r^2 = \left(x + 0.5\right)^2 + y^2 \tag{57}$$

The domain is resolved using a conformal triangulation with 4635 and 9001 elements. For the explicit schemes the integration time step was set to 0.01 s resulting in a CFL number with a maximum value of 0.997 at the boundary of the domain. The maximal and minimal values of the solution for the whole simulation and for the results after one rotation are shown in Table 1. It can be seen that the higher order non-monotone schemes (CRD-LDA. CRD-LAX and CRD-UCV) exhibit negative values during one rotation.

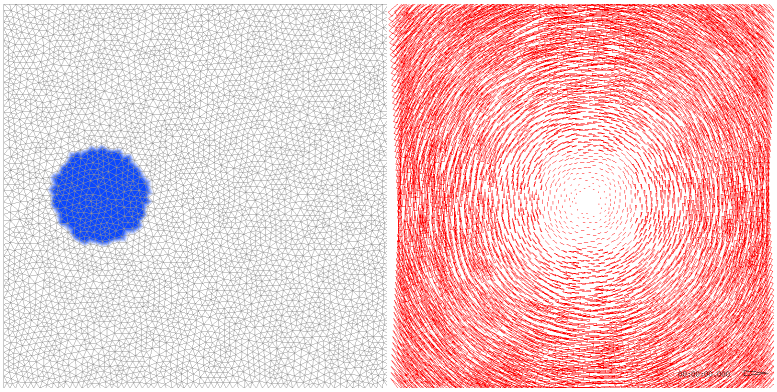

Figure 5: Left: Initial values, analytical solution after one revolution and computational mesh. Right: Velocity distribution according to eq.55.

The CRD-LAX scheme result has pronounced negative values and unwanted maxima after one evolution. The CRD-LDA and the CRD-UCV scheme lead to moderate negative values but are much more dissipative since the peak value after one revolution is reduced to 0.61 and 0.55 respectively. The monotone linear N-scheme is the most dissipative one since half of the peak values is lost after on revolution. The monotone nonlinear CRD-PSI scheme is nearly as dissipative as the CRD-N scheme with a maximum of 0.52 after on rotation. Clearly, the best results are obtained with the CRD-FCT scheme. The maximum is preserved and the negative values occurring are neglectable[4].

	CFL = 1.0					
Numerical Scheme	CRD-N	CRD-LDA	CRD-LAX	CRD-UCV	CRD-PSI	CRD-FCT
Min.value	0.00	-0.14	-4.00	-0.12	0.00	0.00
Max. value	1.00	1.12	1.65	1.11	1.00	1.00
Min. after one rotation	0.00	-0.06	-0.36	-0.03	0.00	0.00
Max. after one rotation	0.49	0.61	1.44	0.55	0.52	1.00

Table 1: Minimum and maximum values of the solution during one rotation and after one rotation for the explicit RD-schemes.

[4] The smallest negative value for the CRD-FCT scheme for this test case was -8.67E-19

The results of the numerical simulation for the cylinder after one revolution using the explicit RD-schemes are plotted in Fig.8. The analytical solution equals in that case the initial one. The results show that the CRD-N-Scheme is the most diffusive one. The numerical diffusion in cross and longitudal direction is considerable. The CRD-LDA scheme reduces the diffusion in cross flow direction and maintains much better the maximum, but the non-monotone character leads to negative values in the solution (e.g. negative wave action). The CRD-LAX scheme results in even stronger negative values than the CRD-LDA scheme, the original distribution is distorted, and the solution is oscillative at the wake of the cylinder. Moreover, there is a kind of phase lag in the solution. The central scheme by Paillere (1995) has very similar characteristics as the CRD-LDA scheme.

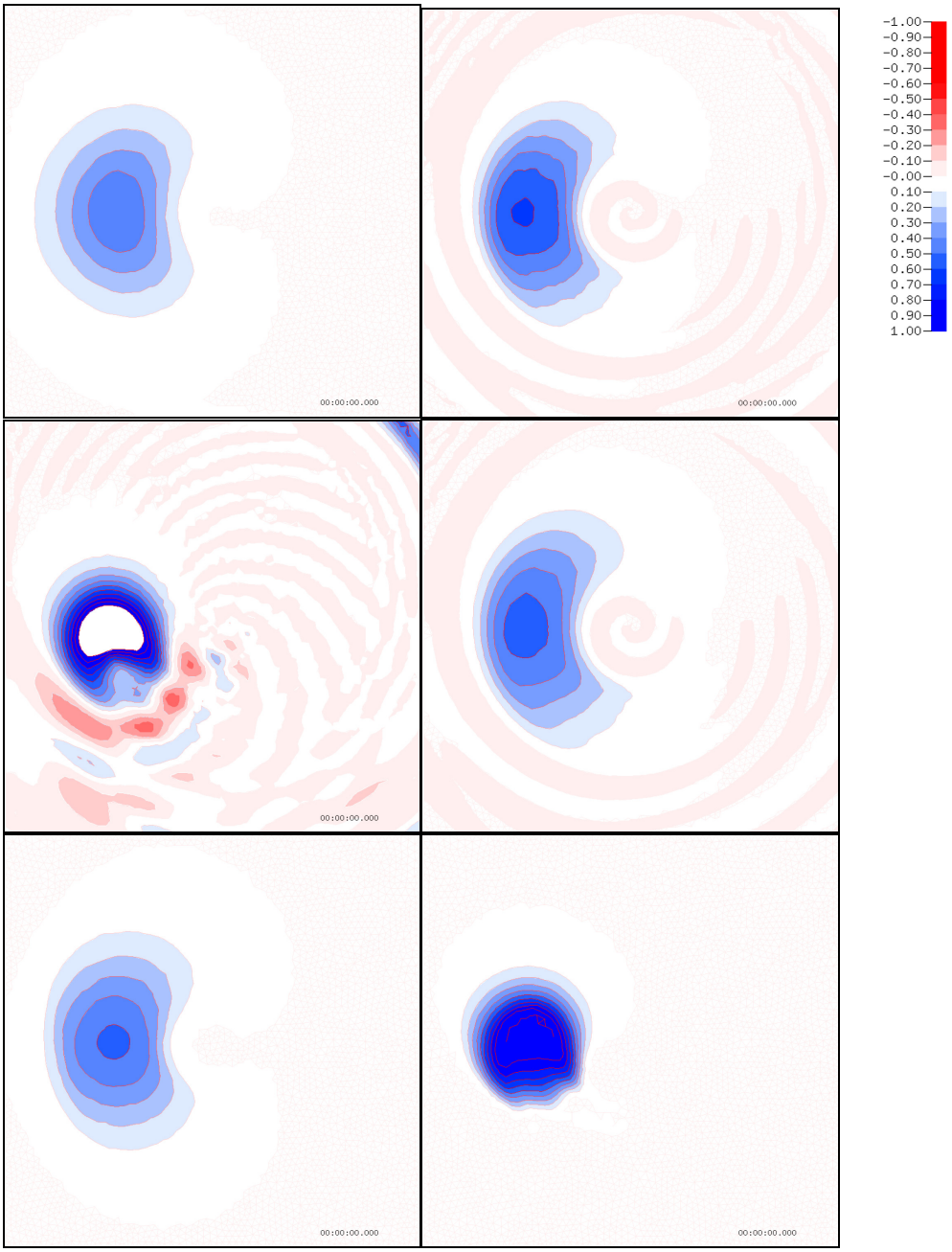

Figure 6: Comparison of the explicit RD-schemes for a rotating cylinder. At the top left: CRD-N-Scheme, top right: CRD-LDA scheme, middle left: CRD-Lax-Wendroff-scheme, middle right: CRD-UVC-scheme, bottom left: CRD-PSI-scheme and at the bottom right the CRD-FCT-FS scheme. Note: Values greater or smaller then the colour scale are not plotted and leaved blank.

The CRD-PSI scheme shows the combination of the results of the CRD-N and CRD-LDA scheme. No negative values but a higher cross diffusion than with the CRD-LDA scheme though smaller than with the CRD-N-scheme. The best results have been obtained with CRD-FCT scheme, which maintains the maximum values also after one revolution.

The phase lag of the CRD-LAX scheme is reduced, but the initial distribution undergoes a deformation during one revolution. In the wake of the cylinder the CRD-LAX solution can still be identified, but the successful reduction of the AEC fluxes results in a positive solution in that region.

2.2.2. Sheltering by Islands

One major benefit of using genuinely unstructured meshes is the flexible discretization of the domain, which makes it possible to discretize even very tiny islands and take in this way in a very elegant way the sheltering into account. Of course on global scale in Deep Ocean, where structured models are still far more efficient and better tested, obstruction maps are the most economic solution to take this into account, but once moved from sub-grid scale to a discrete representation it is of interest to investigate the accuracy of the solution method for the case of sheltering due to islands. The analytical solution is here clear and simple, behind the island there should be zero wave action since there is no diffusion part. The only cross diffusion introduced is the one by the numerical method. Below in Figure 7 a simple unstructured mesh was designed with an island in the middle. The depth is constant 10km and the wave boundary condition is simply described as all energy (Hs = 1m) was put in one bin at a carrier frequency of 0.1 Hz. On the right hand side of Figure 7 the solution, where the white colour indicated 1m significant wave height and the sheltering is shadowing of the islands is then shown by greyscales where black means Hs = 0m. The results reveal that the ideal solution is far from being met by all schemes; however, the influence of the numerical stencil in time and space is clearly visible.

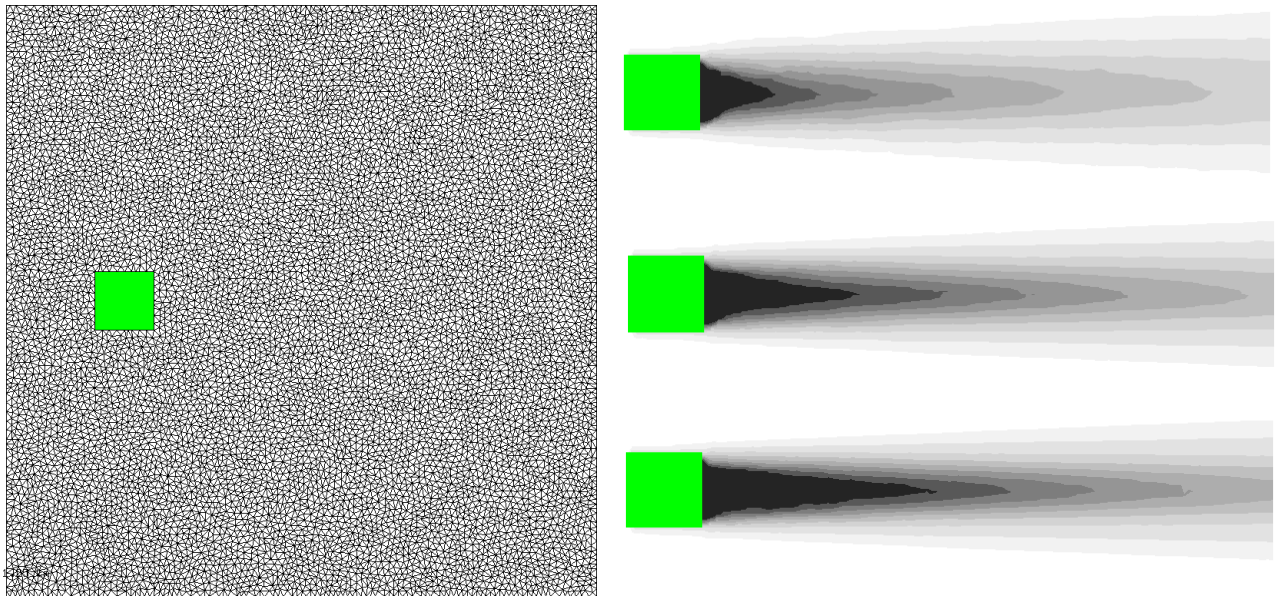

Figure 7: Sheltering by Islands; left: numerical mesh; right top: N-Scheme, right middle: PSI-Scheme, right bottom: LF scheme.

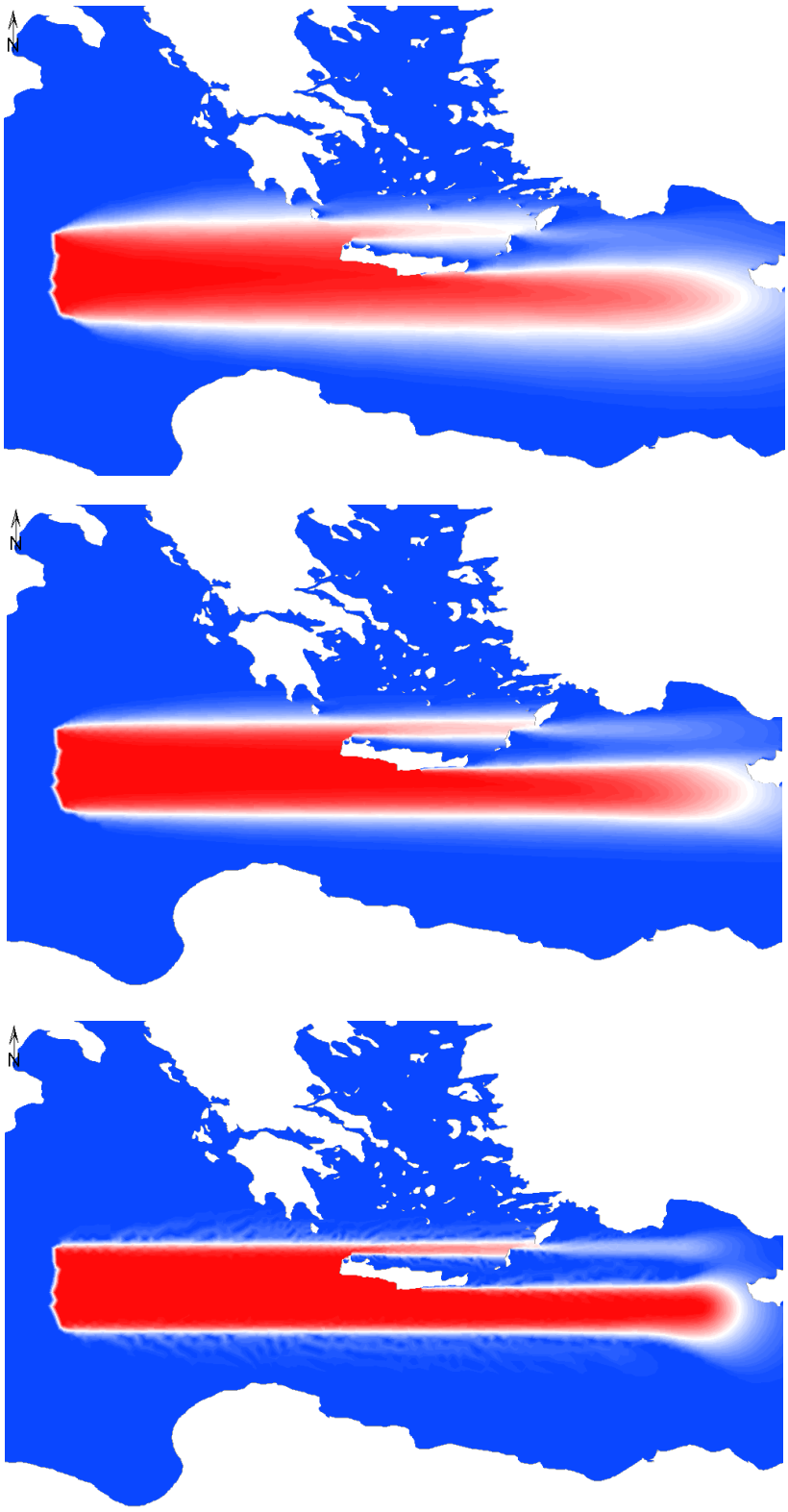

Figure 8: Islands sheltering in the Mediterranean Sea; idealized case. From top to bottom: N-Scheme; PSI-Scheme and LW-Scheme

If there would be some buoys just in the sheltering region, where the variation due to the numerical schemes is pretty high, numerics would have a major impact on the solution. In addition to sheltering

also the penetration depth of wave energy between islands can be a major source of error. Above (Figure 8) a similar case as the idealized one is shown by just putting same wave boundary conditions as used above in the middle of the Mediterranean Sea heading eastward towards Crete (mesh from Figure 1). The sheltering of Crete is clearly visible as well as the influence of the numerical schemes. Another one quite interesting feature in this solution is the penetration depth of wave energy between the Islands of Rhodes and Karpathos. It can be clearly seen that on one hand numerical diffusion results in too little sheltering or wave energy but on the other hand wave energy may not even reach certain places due to diffusion where higher order schemes still do show penetration of wave energy.

2.2.3. Shoaling

Validation of the flux term (2nd term at the right hand side of eq. 29) can be easily done by prescribing a simple bathymetry with linear slope in this case ranging from 20.1m up to 0.1m (the mesh ends at a depth of 0.1m in the last row of elements at the shore; Figure 9) in shallow water at the southern boundary we prescribe similar boundary conditions as above (Hs = 1m, freq. = 0.1Hz) travelling perpendicular to the depth lines. The analytical solution is simply given by solving the flux equation in 1d, which results in terms of Hs

$$H_s = \sqrt{H_{s,i}^2 \frac{c_{g,i}}{c_g}}, \tag{58}$$

where the index i indicates incidence wave condition. All three discretization methods have been compared and the results are shown in terms of relative errors in percent.

$$Err = \frac{H_s - H_{s,analytical}}{H_{s,analytical}} \times 100 \tag{59}$$

The results clearly show the accuracy of the method up to very shallow waters (Figure 10) where quite high gradients in the solution are present (see Figure 10), here the results depend strongly on the discretization but this region is in natural conditions strongly affected by wave dissipation. It can be clearly seen that also for this case the higher order schemes have smaller numerical errors that reduce from 2.7% in case of the CRD-N scheme to 1.5% for the CRD-LW-PSI scheme.

Based on these results it can be said that the implementation of the schemes in validated. In terms of computation performance the PSI scheme is approx. 1.5 as expensive as the N-Scheme and the LW scheme is approx. 2.8 times more expensive than the N-scheme.

From my experience and based on the present representation of the physics in the models, taking into account the lack of modelling diffraction and treating GSE (at least on unstructured meshes) the PSI schemes is the scheme to be used. The implementation of the PSI scheme within the CRD approach using implicit time integrators will be the next step for the author.

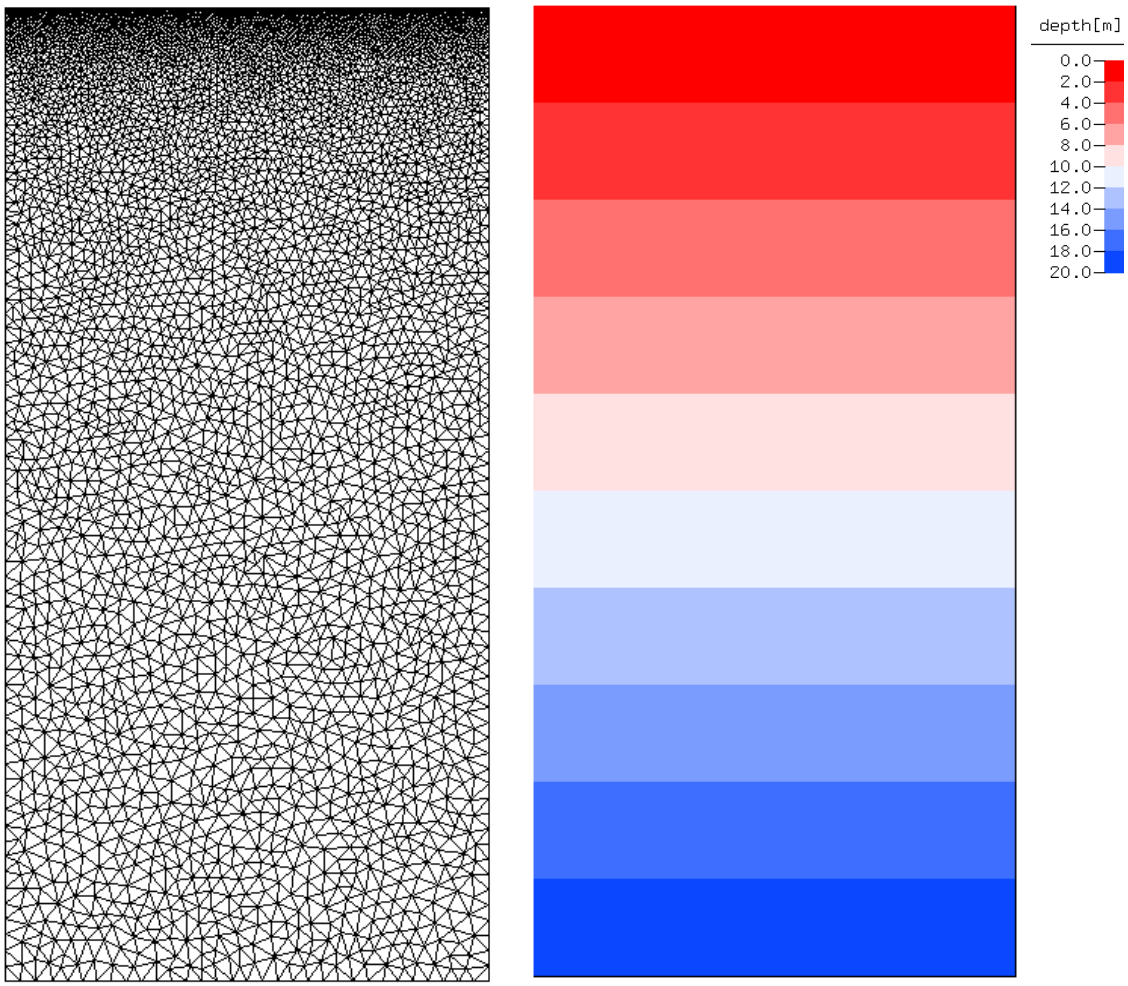

Figure 9: Left: numerical mesh; Right: depth in the computational domain.

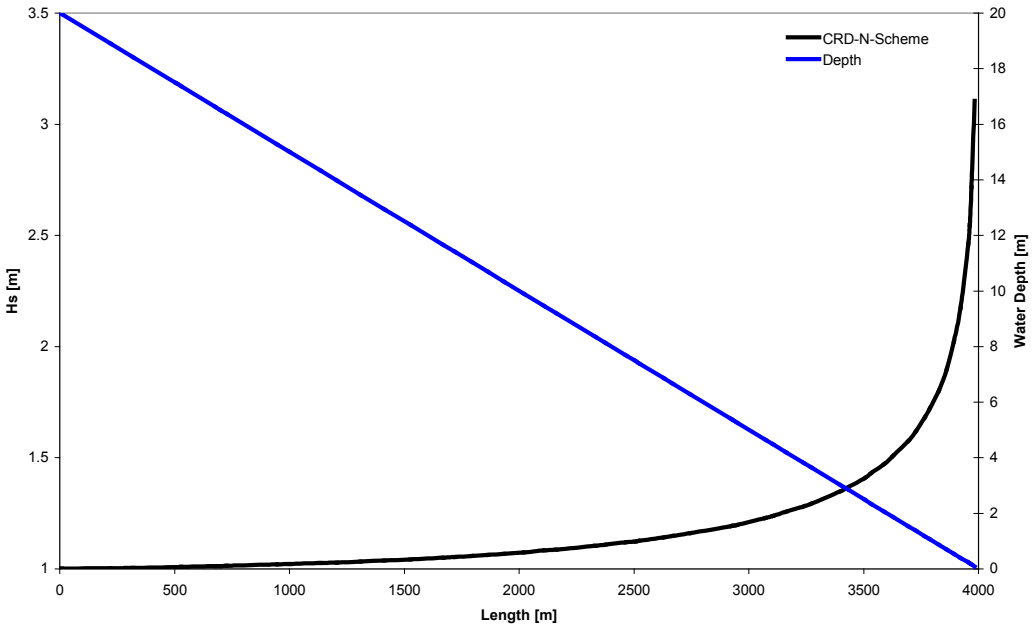

Figure 10: Solution of the WAE for linear depth profile

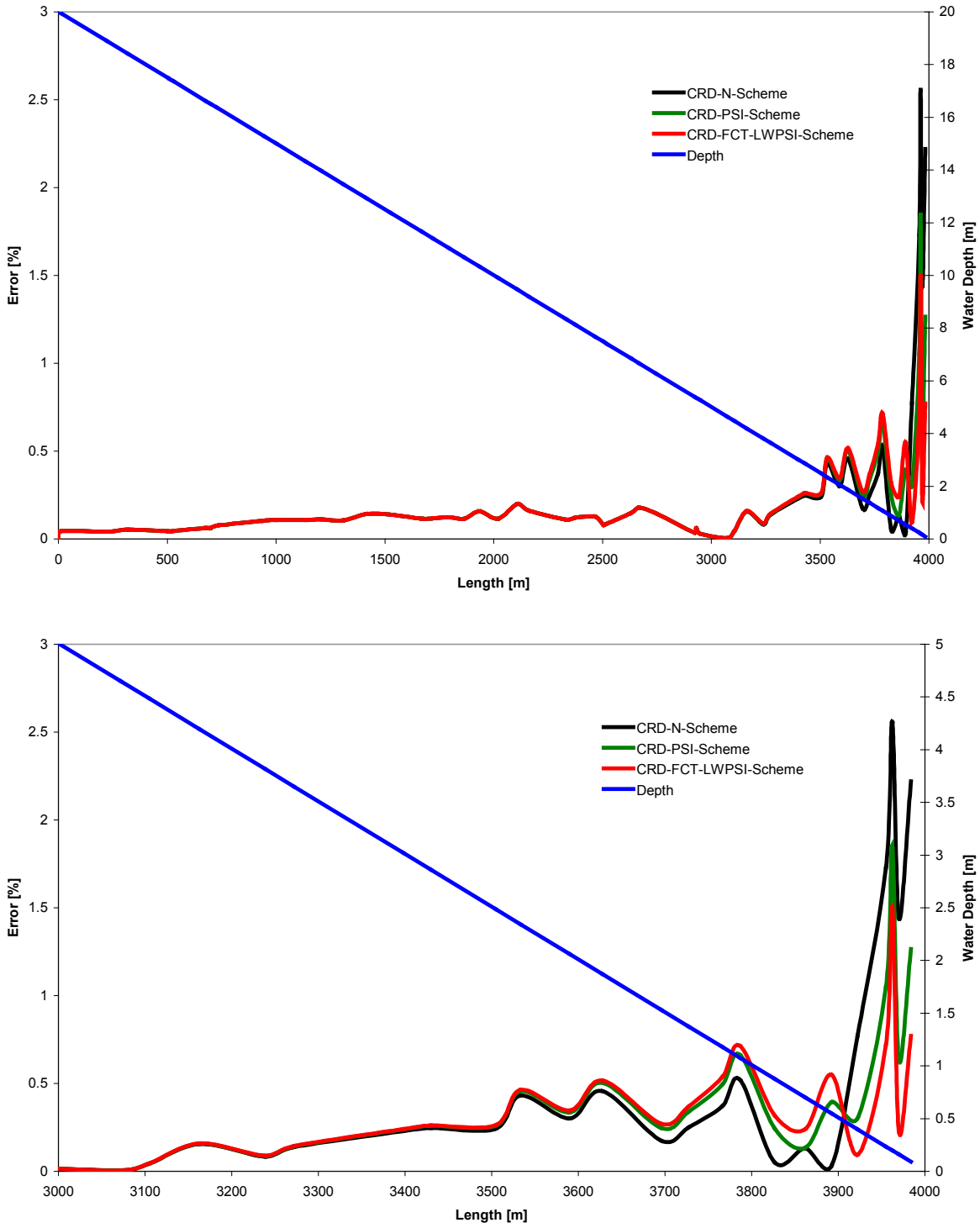

Figure 11: Errors over the whole domain (top) and in the vicinity of the shore (bottom)

3. Outlook and Conclusion

The formalism of RD schemes has been introduced to the WAE. There is no reason why it should be only applied in geographical space, spectral space could be treated as well but since the two operators in spectral space are not commuting, similar to x- and y-space advection, the use of a splitting as done in WW3 is quite nice for spectral space. The problem of splitting the equation and the ongoing errors in splitting remains a problem of most of the implementation (as discussed in Roland, 2009). Another possibility besides the splitting would be, since the RD-schemes are inherently multidimensional, a

non-split solution of the advection part of the WAE on unstructured meshes, which would actually resemble the numerics of the SWAN model but on unstructured meshes. If so, the question of the limiter must be thoroughly investigated since it is not acceptable, that for non-stationary simulations the whole left hand side of the equation becomes limited only because we cannot linearize all source terms properly (remember: Patankar's Laws, that say that proper linearized 1st order schemes are unconditionally stable). Moreover, the stiff contributions of the different terms may result in large Eigenvalues in the matrix resulting in ill-conditioned systems. Therefore A-stable schemes need to be used and a proper numerical framework has to be implemented.

However, here are not only numerical issues to be taken into account but of course also physical as e.g. wave diffraction, which will in a certain way result in cross diffusion of wave energy in the shadowing region of islands. From my point of view it is not a proper approach to approximate physics by numerical errors but this is and will stay reality to certain extend also in the next decade.

This statement is of course highly idealistic but progress and physics must go hand in hand with improved numerical math otherwise the remaining parameters of the partly empirical physical processes depend to a certain extend on the numerical schemes.

References

Abgrall, R. and Roe, P.L., 2003. High order fluctuation schemes on triangular meshes. J. Sci. Comput., 19(1-3), 3–36.

Abgrall, R., 2001. Toward the ultimate conservative scheme: following the quest. J. Comput. Phys., 167(2), 277–315.

Abgrall, R., Mezine, M., 2003. Construction of second order accurate monotone and stable residual distribution schemes for unsteady flow problems, J. Comput. Phys. 188, 16–55.

Abgrall, R. Residual distribution schemes: current status and future trends. Computer and Fluids, 35(7):641--669, 2006. invited paper

Ardhuin, F., 2001: Swell across the continental shelf. Ph.D. thesis, Naval Postgraduate School, 133 pp.

Benoit, M., F. Marcos and F. Becq. 1996. Development of a third generation shallow-water wave model with unstructured spatial meshing, Proceedings of 25th International Conference on Coastal Engineering, ASCE, 465–478.

Donea, J., 1984. A Taylor-Galerkin method for convective transport problems. Internat. J. Numer. Methods Eng., 20, 101-120.

Csík, Á., Ricchiuto, M. and Deconinck, H., 2002. A conservative formulation of the multidimensional upwind residual distribution schemes for general non linear conservation laws. Journal of Computational Physics, 179(1), pp 286-31

Hubbard, M. E., Roe, P. L., 2000. Compact high-resolution algorithms for time-dependent advection on unstructured grids. Internat. J. Numer. Methods Fluids 33, 711-736.

Liau, J-M. 2001, A Study of Wind Waves Hindcasting on the Coastal Waters, PhD Thesis, National Cheng Kung University, Tainan, Taiwan

Qian, Q., Stefan, H., G. and Voller, V. R., 2007, A physically based flux limiter for QUICK calculations of advective scalar transport International Journal for Numerical Methods in Fluids Volume 55, Issue 9, Pages: 899-915

Paillere, H., 1995. Multidimensional upwind residual distribution schemes for the Euler and Navier-Stokes equations on unstructured grids. PhD Thesis, Universite´ Libre de Bruxelles, Belgium.

Ricchiuto, M., Csík, Á., Deconinck, H., 2005. Residual distribution for general timedependent conservation laws. J. Comput. Phys. 209 (1), 249–289.

Roe PL. Characteristic-based schemes for the Euler equations. Ann. Rev. Fluid Mech 1986;18:337–65.

Roland, A., (2009), Development of WWM II: Spectral wave modeling on unstructured meshes. Ph.D. thesis, Technische Universit¨at Darmstadt, Institute of Hraulic and Water Resources Engineering.

Tomaich, G.T., 1995. A genuinely multi-dimensional upwinding algorithm for the Navier-Stokes equations on unstructured grids using a compact, highly-parallelizable spatial discretization. PhD thesis, University of Michigan, USA.

Zanke, U.C.E., 2002. Hydromechanik der Gerinne und Küstengewässer (Parey Verlag)

Acknowledgements

The author is indebted to Peter Janssen for giving the author the opportunity to introduce the RD-Framework to the WAM code. The author is thankful to Jean Bidlot for sharing insights of the code and being helpful in a variety of questions. The author also wish to thank the whole centre for providing a professional and warm atmosphere during my stay, especially, I like to thank Dominque Lucas who has helped in many questions of source code development and HPCF usage.